# Global Potential Energy Contour Plots for Chemical Reactions. Multiple Reaction Paths, Bifurcations, and Applicability of Transition-State Theory

### R. A. Marcus

Noyes Laboratory of Chemical Physics, California Institute of Technology, Pasadena, California 91125 (Received: February 27, 1991; In Final Form: April 19, 1991)

A global reduced-dimensional potential energy contour plot is described for the simultaneous representation of reactions  $X_3Y \rightleftharpoons X_2 + XY$ ,  $X_3Y \rightleftharpoons X + X_2Y$ , and  $X_2 + YX \rightleftharpoons X_2Y + X$ , where the X's may be different. The analysis provides some insight into the nature of the transition states, the role of bifurcations, and the applicability of transition-state theory (TST). Recent results of a quantum chemistry calculation for the X = H, Y = O system are discussed in these terms. More generally, some topographical conditions for the inapplicability of TST are suggested. This limitation of TST arises from a preempting of the transition state for one reaction by another and appears to be relatively rare.

#### 1. Introduction

For visualizing chemical reaction mechanics or distortions of molecular structure, potential energy contour plots have been very helpful. Examples include the common textbook<sup>1</sup> plot with two internal coordinates, used to discuss a collinear treatment of the triatomic exchange reaction (1), as in Figure 1

$$R + BC \rightarrow AB + C \tag{1}$$

and systems with three or more coordinates but with all coordinates but two held constant in the diagram, as in a common pictorial description of the Jahn-Teller distortion of an electronically degenerate molecule such as Na<sub>3</sub> or Cu<sub>3</sub> from an equilibrium triangular configuration.<sup>2</sup> The latter is shown in Figure 2, where the symmetric stretching coordinate is held fixed.

A third example is the previous system, but now with the remaining coordinates varied so as to minimize pointwise the potential energy.<sup>3</sup> The plot is again similar in appearance to Figure 2. In this figure, as well as later in Figure 3, two suitable coordinate axes are the two asymmetric stretches of this triatomic system. A fourth and related example is that depicted in Figure 3 for a reaction of the type  $X + X_2 \rightarrow X_2 + X$  involving isotopic scrambling, proceeding either via a direct reaction or via an actual intermediate  $X_3$ . In either case the pointwise change in the symmetric stretching coordinate becomes extremely large, as discussed later. A figure such as Figure 3 has been used in a discussion of the  $O_3$  reaction system.<sup>3</sup>

In the present paper we treat in this global way more complicated reaction systems, having several reactions rather than just one:

$$X_3Y \to X + X_2Y \tag{2}$$

$$X_3Y \to X_2 + XY \tag{3}$$

and

$$X_2Y + X \to XY + X_2 \tag{4}$$

In the present discussion the three X's need not be the same. When they differ the initial  $C_{3v}$  symmetry is modified, as are the two asymmetric stretching and other modes, but the principal topographical and related considerations remain the same.

In a recent electronic structure calculation for X = H and Y = O, the transition states for reactions 2 and 4 were located, but not that for reaction 3.<sup>4</sup> When the isotopically different possibilities are considered, there are, in all, some 12 reaction paths to be represented in the diagram. An aim of the present article is to depict reactions such as (2)–(4) in such a way as to provide an overall view of their relationships. The contour plot is then used to explore the location of the transition states and of any bifurcations and to consider whether conventional transition-state theory, with statistical factors added, is even applicable to all of the reactions in such a system.

In section 2 a description of the X<sub>3</sub> reaction system is first recalled. A treatment of reactions 2-4 for the X<sub>3</sub>Y system is described in section 3 and applied to the H<sub>3</sub>O system in section 4. Three-dimensional contour plots are also briefly considered there. Topographical conditions for the applicability or inapplicability of transition-state theory to any particular reaction scheme are considered in section 5. They are illustrated in section 6, using the results in section 4, and examples of multiple reaction path systems where conventional transition-state theory are given. It is also shown in section 6 that if there are any substituents where the two-step and radical intermediate mechanisms, in "synchronous" type reactions, e.g., Diels-Alder, become competitive, complications in application of TS theory would arise for one type of contour plot but not for another.

### 2. X<sub>3</sub> Reactions

We consider here the isotopic exchange reaction

$$X^{(1)} + X^{(2)}X^{(3)} \rightarrow X^{(1)}X^{(2)} + X^{(3)}$$
 (5a)

$$\to X^{(1)}X^{(3)} + X^{(2)} \tag{5b}$$

the superscripts labeling the atoms.

Two suitable coordinates that provide a global picture in the potential energy contour plot are the pair  $(S_{A1}, S_{A2})$  of degenerate asymmetric stretching coordinates. Bond lengths for this system, denoted by  $r_1$ ,  $r_2$ , and  $r_3$ , can be defined for the  $X_3$  system, as in Figure 4a, and orthonormal symmetry coordinates  $S_i$  can be introduced as in Figure 5.

$$S_{\rm S} = \frac{1}{\sqrt{3}}(r_1 + r_2 + r_3), \quad S_{\rm A1} = \frac{1}{\sqrt{6}}(2r_1 - r_2 - r_3),$$
 
$$S_{\rm A2} = \frac{1}{\sqrt{2}}(r_2 - r_3) \quad (6)$$

In a schematic plot of the potential energy contours for reactions 5a and 5b given in Figure 3, the symmetric stretching coordinate  $S_S$  is adjusted pointwise, so as to minimize the potential energy at each value of  $(S_{A1}, S_{A2})$ . The resulting behavior of  $S_S$  in any third of the plot can be obtained from one of the other thirds by rotating about the origin through 120° or 240°.

The assignment of each of the three channels in Figure 3 to the three configurations in eqs 5a and 5b is readily deduced from eq 6, e.g., as in Appendix A, and  $S_S$  is readily seen there to undergo

<sup>&</sup>lt;sup>†</sup>Contribution No. 8399.

<sup>(1)</sup> E.g.: Glasstone, S.; Laidler, K. J.; Eyring, H. The Theory of Rate Processes; McGraw-Hill: New York, 1941. (2) E.g.: Murrell, J. N. In Quantum Theory of Chemical Reactions;

<sup>(2)</sup> E.g.: Murrell, J. N. In Quantum Theory of Chemical Reactions; Daudel, R., Ed.; D. Reidel: Dordrecht, 1980; Vol. 1, p 161. Bersuker, I. B. The Jahn-Teller Effect and Vibronic Interactions in Modern Chemistry; Plenum: New York, 1984. Zwanziger, J. W.; Whetten, R. L.; Grant, E. R. J. Phys. Chem. 1986, 90, 3298. Cocchini, F.; Upton, T.; Andreoni, W. J. Chem. Phys. 1982, 88, 6068.

Chem. Phys. 1988, 88, 6068.

(3) Varandas, A. J. C. Chem. Phys. Lett. 1987, 138, 455. Morais, V. M. F.; Varandas, A. J. C. J. Chem. Soc., Faraday Trans. 2 1989, 85, 1.

(4) Talbi, D.; Saxon, R. P. J. Chem. Phys. 1989, 91, 2376.

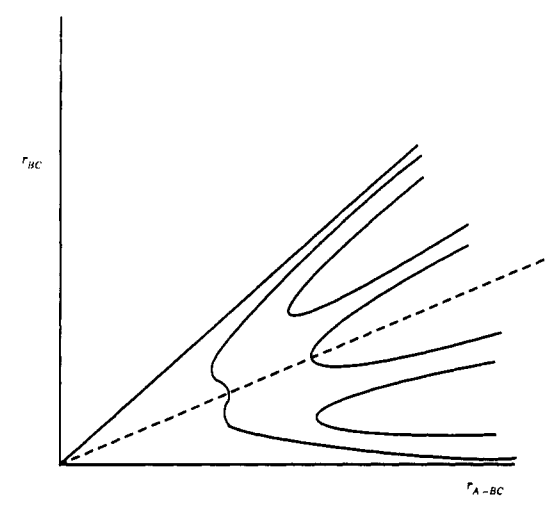


Figure 1. Contour plot for atom abstraction reaction (1).

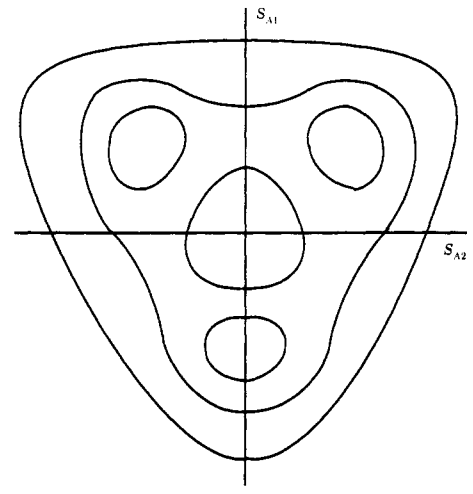


Figure 2. Contour plot for X<sub>3</sub> structural system. The coordinates are the degenerate asymmetric stretches, and the symmetric stretching coordinate is either held fixed or varied so as to minimize the potential energy pointwise. There are three minima and, in the central part, a high region (a conical intersection in ref 2).

an infinite variation as reaction 5 proceeds.

#### 3. X<sub>3</sub>Y Reactions

We consider next a system of principal interest here, namely, reactions 2-4. In the nonlinear X<sub>3</sub>Y system there are six internal coordinates, as in Figure 4b. The symmetry coordinates for a  $C_{3\nu}$ arrangement of X<sub>3</sub>Y (e.g., when it is a trigonal pyramid), depicted in Figure 6, include the XY symmetric stretch  $S_S$  and the degenerate pair of asymmetric XY stretches  $S_{A1}$  and  $S_{A2}$ , all again given by eq 6. There are also a symmetric  $X_3$ Y bend  $S_S$ B and a degenerate pair of XYX bending coordinates  $S_{A1}$ B and  $S_{A2}$ B, as in eq 7 and Figure 6. The six normal modes of this system

$$S_{S}^{B} = \frac{1}{\sqrt{3}}(\alpha_{1} + \alpha_{2} + \alpha_{3}), \quad S_{A1}^{B} = \frac{1}{\sqrt{6}}(2\alpha_{1} - \alpha_{2} - \alpha_{3}),$$
$$S_{A2}^{B} = \frac{1}{\sqrt{2}}(\alpha_{2} - \alpha_{3}) \quad (7)$$

consist of two linear combinations of  $S_S$  and  $S_S^B$ , two of  $S_{A1}$  and  $S_{A1}^B$ , and two of  $S_{A2}$  and  $S_{A2}^B$ , the proportions depending on the force constants and masses.

The desired two-dimensional potential energy contour plot for the system of reactions 2-4 is one containing all paths for that reaction. The contour plot for the case that only reaction 2 occurs is given in Figure 7. In this schematic plot the potential energy has been minimized pointwise with respect to  $S_S$  and the remaining three coordinates. The behavior of  $S_S$  in the vicinity of the three principal paths in Figure 7 is described in Appendix B, together

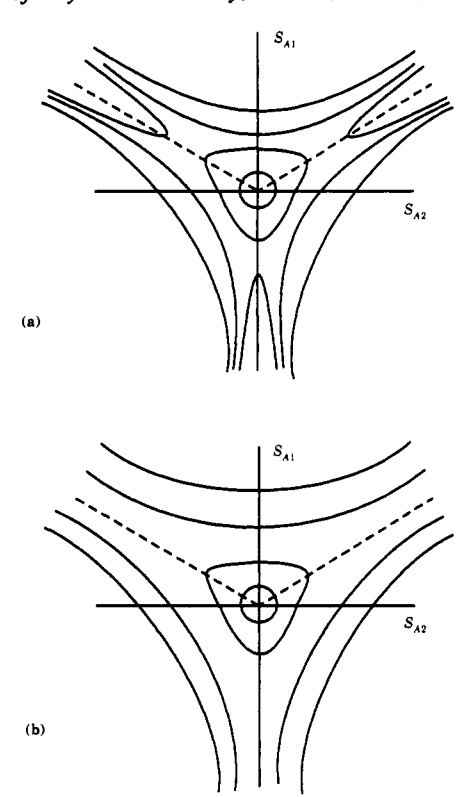
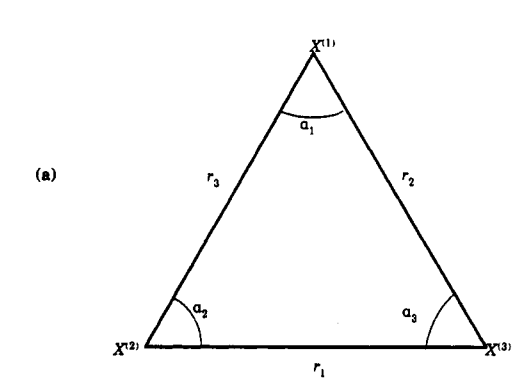


Figure 3. A contour plot for reaction 5: (a) the saddle points are in each exit valley: (b) there are no saddle points and so no hump in each exit valley.



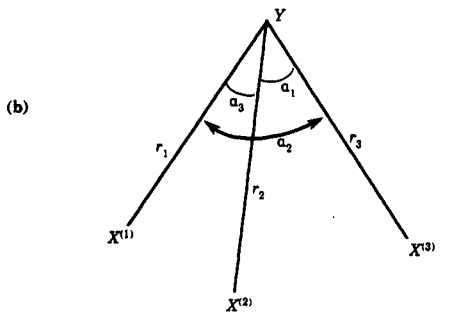


Figure 4. Internal coordinates for the  $X_3$  and  $X_3Y$ . The three angles  $\alpha_i$ in (a) are redundant when, as in eq 6, the  $r_i$ 's are used.

with the behavior along radii leading to the products of reaction

An example where all three reactions (2)-(4), occur is given in the next section, where we consider a particular example of the X<sub>3</sub>Y system, H<sub>3</sub>O.

### 4. Dissociations of H<sub>3</sub>O and Abstraction Reaction HO + H<sub>2</sub>

In a recent quantum mechanical study, calculations were made for the system of reactions 2-4 where  $\dot{X} = H$  and Y = O.4 One

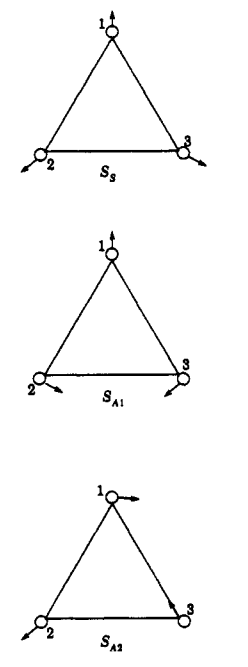


Figure 5. Normal modes for the  $X_3$  system.

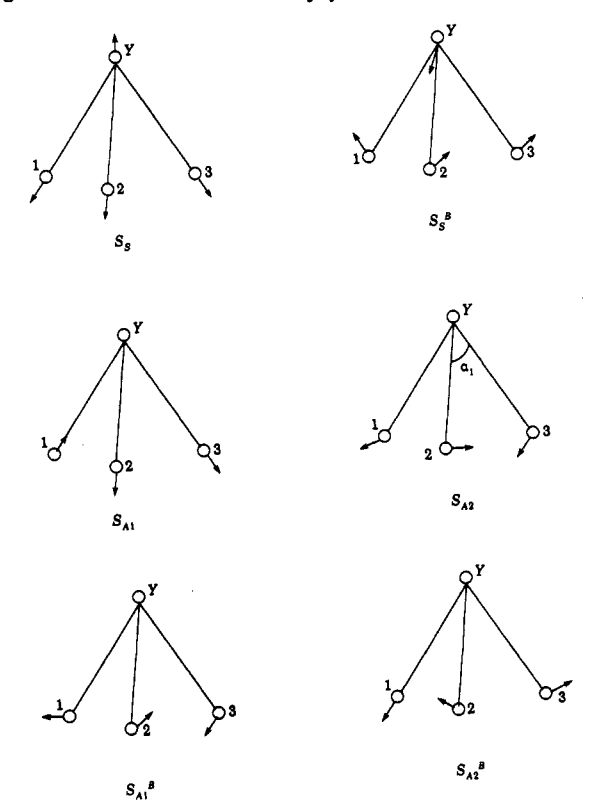


Figure 6. Symmetry coordinates for  $X_3Y$ .

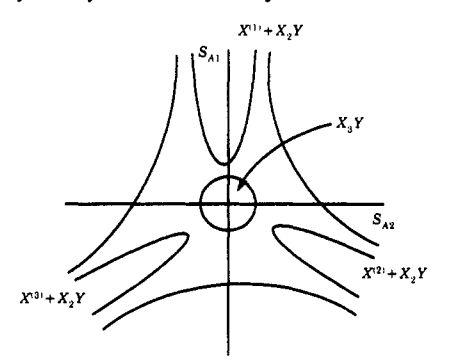


Figure 7. Contour plot for reaction 2.

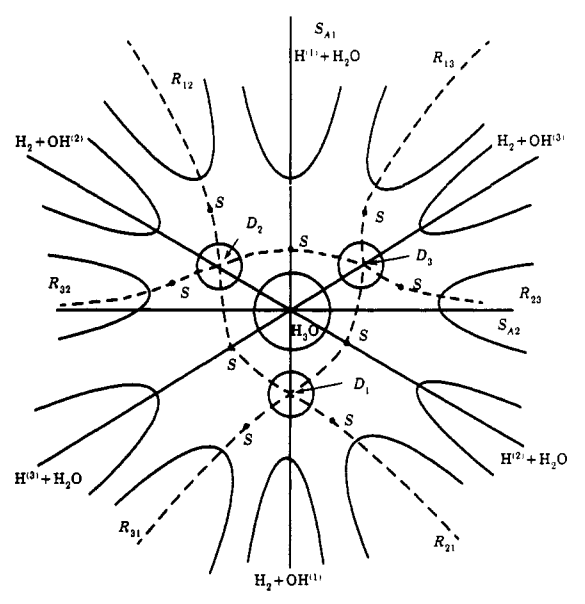


Figure 8. Contour plot for reactions 2-4.

possible global two-dimensional potential energy plot, motivated by some inferences from that quantum chemical study, is given below.

Two dissociation paths of H<sub>3</sub>O are

$$H_3O \rightarrow H + H_2O$$
 (8)

and

$$H_3O \rightarrow H_2 + HO$$
 (9)

The abstraction reaction

$$H_2 + HO \rightarrow H + H_2O \tag{10}$$

was also studied. The fact that  $H_3O$  only had a very shallow well in the study does not affect the illustration itself but would bear on the observability of the  $H_3O$ . One could also consider, instead, therefore, the case where  $YX_3$  is a stabler entity, such as  $NH_3$  or  $PH_3$ . In the following and later in section 6 the transition state will frequently contain a saddle point, but in cases such as some unimolecular dissociations that have no local "hump", along their reaction path, as probably in reaction 8 and as in Figure 3b, the transition state is determined variationally (variational TS theory). The lowest point for each TS is nevertheless denoted by S, which may, or may not, be an actual saddle point.

The transition state for reactions 8 was located in ref 4, while that for reaction 10 was located earlier, 5 but the one for reaction 9 was not found. Instead, a dome was located on the potential energy surface, tending to block a normal-mode path leading from  $H_3O$  to  $H_2 + HO$ . That normal-mode path was not the sought for reaction path, since there would be a lower energy path around the dome. It was found that, on proceeding in each of four directions from the top of that dome, certain molecular species were observed. A set of potential energy contours which we find is consistent with those observations is given in Figure 8. In this schematic plot  $S_S$  and the remaining three coordinates are allowed to vary pointwise with  $(S_{A1}, S_{A2})$  so as to minimize the potential energy

In Figure 8 there are three domes  $D_i$  (i = 1-3) and a shallow bowl occupied by and denoted by  $H_3O$ . Six ridges  $R_{ij}$  separate six valleys, the i referring to the  $H^{(i)}$  valley for reaction 11 and the j to the OH<sup>(j)</sup> valley for reaction 12. The method used to establish the species in each of these valleys is based on eq 6 in the previous section.

<sup>(5)</sup> Walch, S. P.; Dunning, T. H. J. Chem. Phys. 1980, 72, 1303. Dunning, T. H.; Kraka, E.; Eades, R. A. Faraday Discuss. Chem. Soc. 1987, 84, 427. Schlegel, H. B.; Sosa, C. Chem. Phys. Lett. 1988, 145, 329. Cf.: Kochanski, E.; Flower, D. R. Chem. Phys. 1981, 57, 217.

$$H_3O \to H^{(i)} + H_2O$$
 (11)

$$H_3O \rightarrow H_2 + H^{(j)}O \quad (j = 1, 2, 3)$$
 (12)

There are several dashed lines which join domes to domes or a dome to its two nearby ridges. They denote the paths of steepest ascent along the transition state to the ridge or to the apex of the dome. They serve as the transition states for nine of the reactions. The nine points S are situated at the lowest points of potential energy on the relevant parts of the transition states.

In Figure 8, the transition state for the dissociation of H<sub>3</sub>O into  $H^{(2)} + H_2O$  is the dashed line joining  $D_1$  to  $D_3$ . The transition state for the abstraction reaction  $H_2 + OH^{(1)} \rightarrow H^{(2)} + H_2O$  is the dashed line joining ridge  $R_{21}$  to dome  $D_1$ .<sup>6</sup> Similar remarks apply to the other symmetrically related reactions (permutations of the superscripts). Each dome D inhibits the system from proceeding on a straight-line reaction path from the H<sub>3</sub>O bowl to the  $H_2 + OH^{(l)}$  products (e.g., along the negative  $S_{A1}$  axis, for

Not shown are lines that pass from valley to adjacent valley through the same points S, but at right angles to the existing dashed line at that S. This second set of lines corresponds to the minimum-energy paths between two valleys (e.g.,  $H_2 + OH^{(1)}$  and  $H^{(2)} + H_2O$ ), the "intrinsic reaction paths". There are six such valley-to-valley paths passing through the relevant six saddle points S for the six permutations of i and j ( $i \neq j$ ) in the H<sub>2</sub> + OH<sup>(i)</sup>  $\rightarrow$  H<sup>(f)</sup> + H<sub>2</sub>O reaction.

In the case of the dissociation of  $H_3O$  into  $H_2 + OH^{(1)}$  (or other permutations) the minimum-energy reaction path for this dissociation is not over the intervening dome 1, since as already noted there are lower energy paths around the dome. Indeed, there is not in Figure 8 a conventional transition state for this reaction, a point to which we return shortly. Examining Figure 8 and the role of the dome, it is seen that in the formation of  $H_2 + OH^{(1)}$ from H<sub>3</sub>O, the mechanism does not occur via a symemtric dissociation along the negative  $S_{A1}$  axis, in which two H's would depart symmetrically from the HO along the OH axis, the  $S_S$ continually readjusting in such a motion, and the H's simultaneously approaching each other to form H<sub>2</sub>. Such a motion involves going over the dome instead of on a lower-energy path around it. Thus, the dissociation first involves an asymmetric motion of the departing two H's of H<sub>3</sub>O that ultimately form H<sub>2</sub>, much as in the dissociation of  $H_2CO$  to  $H_2 + CO$ , and perhaps for a similar reason, namely to circumvent an orbitally forbidden nature of a symmetric dissociation in this system.

We turn now to the missing transition state for the  $H_3O \rightarrow H_2$ + OH reaction. The problem, if the surface in Figure 8 is qualitatively correct, arises because of a bifurcation there, and we consider this aspect next. A classic example of a bifurcation is the monkey saddle, a saddle point with three routes of steepest descent from the saddle point, instead of the two for the conventional saddle point.<sup>8</sup> More typically, however, bifurcations are not expected to coincide with the transition state itself,9 except in some system of appropriate symmetry. To have only the bifurcation it suffices merely that there be three low regions on the potential energy surface, separated by three high regions. In the case of the reactions in Figure 8 we have schematically blown up a portion, as in Figure 9. In this figure in a 120° sector the three low regions are the  $H_3O$  bowl (one-third of it) and the  $H_2 + OH^{(1)}$ and H<sup>(2)</sup> + H<sub>2</sub>O valleys. The three high regions separating the three low ones are the dome  $D_1$  and the ridges  $R_{21}$  and  $R_{31}$ . This type of bifurcation can be termed a "tilted monkey seat on the side of a hill". It differs from a monkey saddle in that the latter

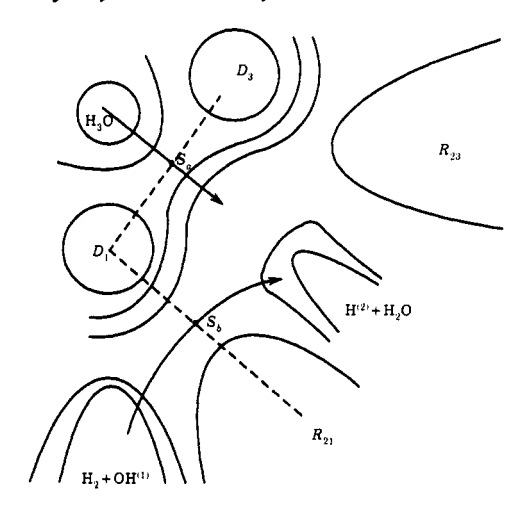


Figure 9. Enlargement of a sector of Figure 8.

has a zero slope at the bifurcation point.

The transition state (TS) for the  $H_3O \rightarrow H^{(2)} + H_2O$  reaction contains the point  $S_a$  in Figure 9, while that for the  $H_2 + OH^{(1)}$ +  $H_2O$  reaction has a saddle point  $S_b$ . Thus, the "transition state" for the  $H_3O \rightarrow H_2 + OH^{(1)}$  reaction has already been preempted by the other two reactions. Indeed, leaving the H<sub>3</sub>O bowl by crossing the TS containing  $S_a$  the system must proceed on the side of a hill in order to reach the preempted TS containing  $S_b$  and, thereby, reach the  $H_2 + OH^{(1)}$  valley. Clearly, because of the preempting, conventional transition-state theory will not permit a calculation of such a rate constant. Unlike most of the reaction systems considered in the next section, simple statistical factors appended to the usual transition-state expression for the rate constant would not suffice in such a calculation. Indeed, because of the largely or partly preempted parts of the transition states, there is probably not only the well-known energy barrier for an orbitally forbidden reaction  $H_3O \rightarrow H_2 + OH$  but also a phase space availability barrier. A classical trajectory calculation of rates for this or related systems would indeed be of interest. Of course, any breakdown of TS theory for this reaction could also cause some breakdown for the other two reactions,  $H_3O \rightarrow H +$  $H_2O$  and  $H_2 + OH \rightarrow H_2O$ , since the TS spaces are no longer 100% allottable to these reactions. If the topography is as depicted in Figure 8, however, such breakdowns for those two reactions could be minor.

An analysis of a model of a potential energy surface which has the three high regions, three low regions, a bifurcation, and two saddle points has been discussed by Hoffman et al., 10 who treat the surface  $U = (xy^2 - yx^2 + x^2 + 2y - 3)/2$ . A portion (onethird) of the surface depicted in the present Figure 8 can be placed in qualitative 1:1 correspondence with Figure 2 of that reference. The simplicity of U there permitted a simple calculation of the various contours and other properties.

The present picture is not expected to be qualitatively altered from that in Figure 8 when a three-dimensional plot is made using coordinates  $(S_S, S_{A1}, S_{A2})$ , instead of the two-dimensional one in Figure 8: The bowl in Figure 8 becomes spherical-like, the "domes" become cylindrical-like objects rising from the  $(S_{A1}, S_{A2})$ plane and the ridges  $R_{ij}$  rise from their base in the  $(S_{A1}, S_{A2})$  plane. The dashed lines in Figure 8 become dashed planes or dashed curved surfaces connecting these high-energy regions  $D_i$  with the  $R_{ii}$ 's and with each other. The bifurcations and points S continue as before. The valleys become shell-like objects, more or less centered about the  $S_S$  vs  $S_R$  lines described in Appendix B, and these lines alternate in their slopes as described there. Thereby, the value of  $S_S$  giving the lowest point on the surface at any particular value of  $S_R$  yields a somewhat foliated curve as one circles the  $S_S$  axis at constant cylindrical radius. Nevertheless, it should be mentioned that a more detailed investigation of the

<sup>(6)</sup> The lowest point on this line is the saddle point, denoted by S. The entire line denotes all configurations of the TS, and the point S, conventionally called the TS, denotes the least unstable of them.

<sup>(7)</sup> Goddard, J. D.; Schaefer, H. F. J. Chem. Phys. 1979, 70, 5117 and references therein.

<sup>(8)</sup> Cf.: Marcus, R. A. J. Chem. Phys. 1964, 41, 610 and references

<sup>(9)</sup> E.g.: Stanton, R. E.; McIver, J. W. J. Am. Chem. Soc. 1975, 97, 3632. Murrell, J. N.; Laidler, K. J. Trans. Faraday Soc. 1968, 64, 371.

<sup>(10)</sup> Hoffman, D. K.; Nord, R. S.; Ruedenberg, K. Theor. Chim. Acta

Figure 10. Doubling of the domes in Figure 9.

potential energy surface may reveal topographical features different from those in Figure 8.

The  $H_3O$  species is not, apparently, a known entity. However,  $NH_3$  is, and so a quantum chemistry investigation of the contour plot for a reaction system such as that for  $NH_3 \rightarrow NH_2 + H$ ,  $NH_3 \rightarrow H_2 + NH$ , and  $H_2 + NH \rightarrow H + NH_2$  would be of interest.

### 5. Conditions for Inapplicability of Transition-State Theory

The limitation on transition-state theory found in the preceding section arises from the preempting of the TS region of one reaction by another. There are numerous cases, however, where this preempting does not occur, and some examples are given in the next section. It is useful to see whether this phenomenon, and hence the inapplicability of TS theory, can be expressed in terms of some topographical conditions. We consider for this purpose, the following conditions for preempting to occur. (1) There are three systems A, B, and C in which the reactions  $A \rightarrow B$ ,  $B \rightarrow C$ , and  $A \rightarrow C$  occur. (2) There are three low regions, associated with A, B, and C, respectively, separated by three high regions. (3) B and C are not symmetrically related, so that it is not possible to relate the rate constant of  $A \rightarrow B$  to that of  $A \rightarrow C$  by symmetry-related considerations.

Reactions 8-10 satisfy all three conditions, and indeed, as seen earlier, TS theory is inapplicable for at least one of the reactions. In the following section we explore examples where in most cases no or only minor preempting occurs, and so TS theory is then applicable. Condition 2 should, of course, be interpreted in terms of the full-coordinate space rather than in just a two-dimensional one. However, the contours in the two-dimensional space may still provide a useful guide.

In the present paper we are concerned with the question of any breakdown of transition-state theory due to the preempting of the transition state, or preempting part of the transition state, of one reaction by another. Two other sources of breakdown are not considered here: one is due to the sluggishness, if any, of the solvent dynamics, affecting the quasi-equilibrium approximation for the TS. When it occurs it is treated by adding a solvent dynamics formalism, the TS aspect often then appearing in a boundary condition in that formalism.<sup>11</sup> In this way the behavior system may vary between the extreme of largely solvent dynamics controlled to largely quasi-equilibrium TS controlled and can be treated. A second source of breakdown, which can be relatively minor in absolute terms but can sometimes be important in investigations of trends such as pressure effects, <sup>12</sup> is associated with

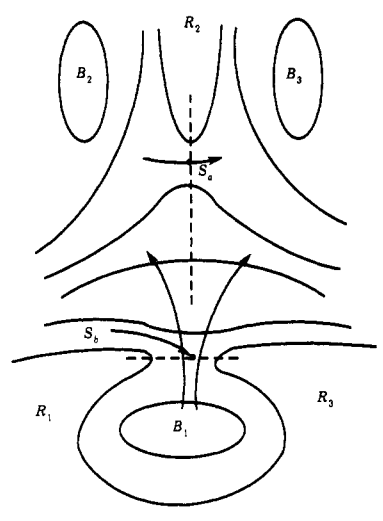


Figure 11. Symmetrical system showing a bifurcation of paths after passage through a transition state (centered at  $S_b$ ).

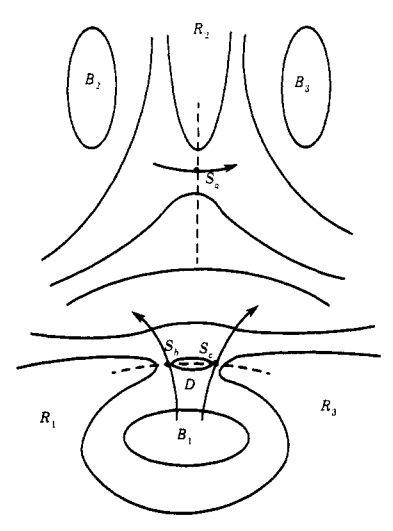


Figure 12. Symmetrical system showing a bifurcation before passage through a transition state (centered at  $S_b$  and  $S_c$ ).

recrossings of the TS, the absence of which, Wigner<sup>13</sup> pointed out many years ago, is needed as one condition for validity of the quasi-equilibrium assumption of TS theory. In the present paper, where the focus is on the potential energy contours themselves, we neglect such kinematic effects.

#### 6. Examples of Other Systems

There are numerous systems where alternative reaction paths are possible and where no preempting of a TS occurs. An example of a change in topography from that in Figures 8 and 9 which would largely eliminate the preempting is the replacement of each blocking dome D by a pair of domes arranged symmetrically about each formerly blocked path, as in Figure 10. Condition 2 is now no longer fulfilled, since in a (somewhat deformed) 120° sector in Figure 10 there are now four high regions,  $D_{1b}$ ,  $D_{3a}$ ,  $R_{12}$ , and  $R_{23}$ , and three low ones, valleys  $V_1$  and  $V_2$  and one-third of a basin. TS theory becomes applicable. The only path that was available for reaction 9 in Figure 9 now becomes in Figure 10 a minor path

<sup>(11)</sup> Recent reviews of some solvent dynamics effects is given in: Weaver, M. J.; McManis, G. E. Acc. Chem. Res. 1990, 23, 294. Bagchi, B. Annu. Rev. Phys. Chem. 1989, 40, 115. An example where a TS expression serves as a boundary condition in the solvent dynamics differential equation and where other coordinates are present is given for electron transfers in: Sumi, H.; Marcus, R. A. J. Chem. Phys. 1986, 84, 4894. Nadler, W.; Marcus, R. A. Ibid. 1987, 86, 3906.

<sup>(12)</sup> E.g., in stochastic molecular dynamics calculations of the chair-boat isomerization of cyclohexane [Kuharski, R. A.; Chandler, D.; Montgomery, J. A.; Rabii, F.; Singer, S. J. J. Phys. Chem. 1988, 92, 3261], a pressure-dependent (viscosity-dependent) transmission coefficient in solution in the neighborhood of 0.5 was found due to recrossings. In an  $S_{\rm N}2$  reaction  $C^{\Gamma}$ +  $CH_3CI$  —  $CICH_3$ +  $CI^{\Gamma}$  [Gertner, B. J.; Wilson, K. R.; Hynes, J. T. J. Chem. Phys. 1989, 90, 3537] a computer simulation molecular dynamics calculation gave a transmission coefficient of about 0.5 due to recrossings. While these factors are not major ones, when compared with other uncertainties in TS theory calculations, they should be taken into account when relatively small trends are measured, such as the effect of pressure on reaction rates in solution. (13) Wigner, E. Trans. Faraday Soc. 1938, 34, 29.

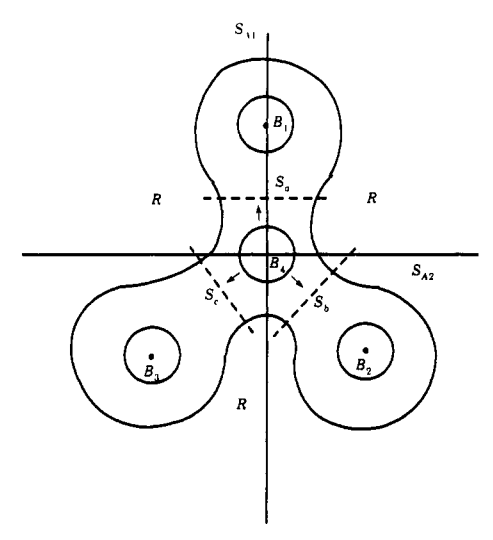


Figure 13. Contour plot for reaction 15.

relative to the direct path which has opened up between  $D_{1a}$  and  $D_{1b}$  for that reaction.

Other examples of a bifurcating system are those given in Figures 11 and 12. If the topography is such that each trajectory leaving  $B_1$  to the left ends up only on the basin on that side, i.e., that none reach, instead,  $B_3$  by crossing the TS indicated by the vertical dashed line, TS theory is applicable. In a symmetric situation (violation of condition 3) such crossings would occur equally, and because of purely statistical considerations TS theory could still be employed. When the dome D in Figure 12 is high and wide enough, it reduces the possibility of such trajectories. There are then four high regions,  $R_1$  to  $R_3$  and D, and three lows,  $B_1$  to  $B_3$ , so that condition 2 of section 5 is not fulfilled and TS theory again applies, regardless of whether or not condition 3 is violated.

A system similar to Figure 12 has been described by Valtazanos and Ruedenberg<sup>14</sup> for the reaction from cyclopropylidene to allene

$$\begin{array}{c}
\ddot{C} \\
H_2C - CH_2
\end{array} \longrightarrow H_2C = C = CH_2$$
(13)

In their plot (Figure 12 of ref 12) the two coordinates used were a ring-opening angle and the mean of the two dihedral angles between each of the CH<sub>2</sub> planes and the CCC plane.

Another example involves the isomerization of the methoxy radical15

$$CH_3O \rightarrow CH_2OH$$
 (14)

the course of the reaction being described by

$$H^{(1)}$$
 $H^{(2)}$ 
 $C-O$ 
 $H^{(2)}$ 
 $H^{(3)}$ 
 $H^{(3)}$ 

An antisymmetric pair of CH stretching coordinates for the three H's, and a symmetric CH stretch, can be introduced (eq 6) and the potential energy plotted as a function of  $S_{A1}$  and  $S_{A2}$ , after minimization with respect to all other coordinates. The resulting contour plot would resemble Figure 13. The basin  $B_4$  corresponds to  $H_3CO$ , and the basins  $B_1$  and  $B_3$  correspond to the three configurations of  $H_2COH$  in reaction 15, where an  $H^{(l)}$  is attached to the O, with i = 1-3. In Figure 13 there is a conventional transition state for each of these three dissociation paths. There are seen to be four low regions B and three highs, R, and so condition 2 is again not fulfilled. TS theory is applicable for the reactions indicated.

In one dissociation studied<sup>7</sup>

$$H_2CO \rightarrow CO + H_2$$
 (16)

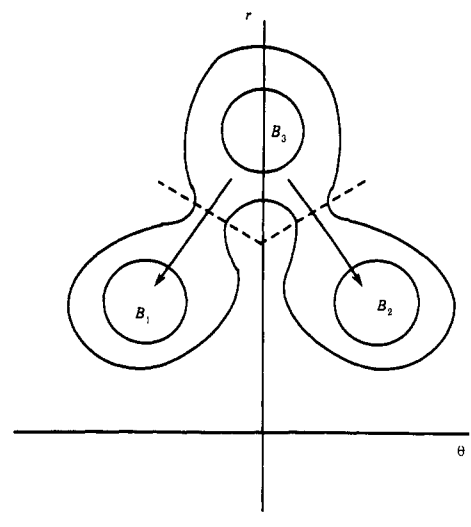


Figure 14. Contour plot for reaction 17.

other reaction products such as H + HCO occurred at substantially higher energy and so did not interfere in the study. The reaction was found in a quantum calculation<sup>7</sup> to proceed via a bent configuration of the TS:

If as one coordinate for a contour plot an angle  $\theta$ , the angle between the bisector of the  $H^{(1)}CH^{(2)}$  angle and the positive CO axis, is used ( $\theta$  can be positive or negative) and if the  $H^{(2)}H^{(1)}$ distance r is chosen as a second coordinate, a schematic plot describing reaction 17 is that given in Figure 14.  $B_3$  corresponds to the reactant, and  $B_1$  and  $B_2$  correspond to the two symmetrically related product configurations in reaction 17. (Only one is shown in reaction 17.) Once again, conventional transition-state theory suffices. For reaction 17 and Figure 14 condition 1 is not fulfilled.

An example where there are two sets of reactions is the dissociation and the isomerization of H<sub>2</sub>CS<sup>16</sup>

$$H_2CS \rightarrow H_2 + CS$$
 (18)

$$H_2CS \rightarrow HCSH$$
 (19)

the course of which can be represented as16

$$H^{(1)}$$
 $C-S$ 
 $H^{(2)}$ 
 $C-S$ 
 $H^{(2)}$ 
 $C-S$ 
 $C-S$ 
 $C-S$ 
 $C-S$ 
 $C-S$ 

and

$$H^{(1)}$$
  $C-S$   $H^{(2)}$   $C-S$   $H^{(2)}$   $H^$ 

As global coordinates the coordinates  $\theta$  and r used in Figure 14 may again be employed, yielding the schematic diagram of the potential energy contours given in Figure 15. Examining the right half of that figure, it is seen that condition 1 is not fulfilled in the quantum mechanical study, there being only two instead of three reactions.

An interesting series of reactions that may occur either concertedly or in a nonconcerted (two-step) manner were reviewed recently by Borden et al.<sup>17</sup> They include the Cope rearrangement,

<sup>(14)</sup> Valtazanos; Ruedenberg, K. Theor. Chim. Acta 1986, 69, 281.
(15) Coiwell, S. M.; Handy, N. C. J. Chem. Phys. 1985, 82, 1281.

<sup>(16)</sup> Tachibana, A.; Okazaki, I.; Koizumi, M.; Hori, K.; Yamaba, T. J. Am. Chem. Soc. 1985, 107, 1190.

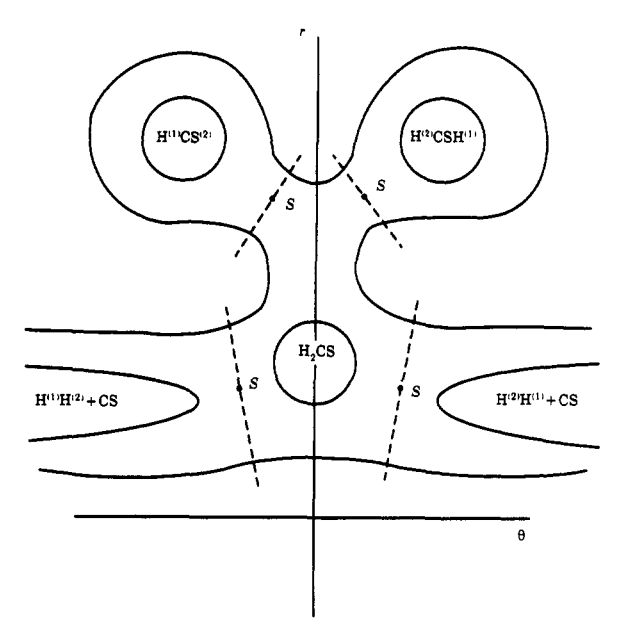


Figure 15. Contour plot for reactions 20 and 21. The angle  $\theta$  is defined in the text. In the  $H_2 + CS$  products' regions the contours are seen to become independent of  $\theta$ .

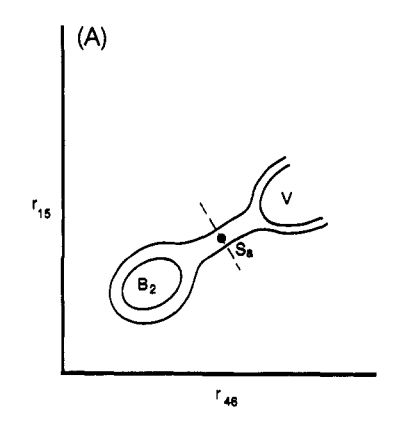
the Diels-Alder reaction, the Alder ene reaction, and the 1,3-dipolar cycloaddition, among others. We consider the Diels-Alder reaction as more or less prototypical. There are several possible mechanisms, <sup>17</sup> considered below: reaction 22 which is a concerted mechanism, reaction 23 which is a two-step mechanism proceeding via a diradical intermediate, and reaction 24 which is concerted mechanism having an unsymmetrical transition state.

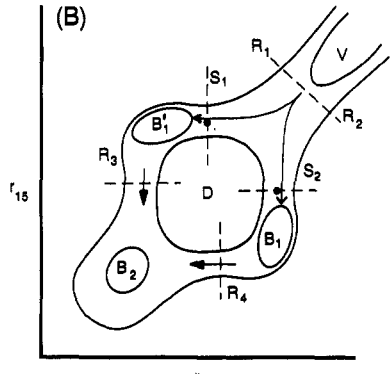
As coordinates we may use the 1-5 distance  $r_{15}$  and the 4-6 distance  $r_{46}$ . The  $r_{23}$  distances in the TS in reaction 22 and in  $B_1$  in reaction 23 are about equal. Three of the possible topographical contour plots are given in Figure 16A-C for reactions 22-24, respectively. Here V,  $B_1$ , and  $B_2$  refer to the compounds indicated in reactions 22-24, and  $B_1'$  is the symmetrically related isomer of  $B_1$  having the 1-5 bond instead of the 4-6 one.

In the case of reactions 22–24 there is only one final product, apart from possible stereoisomers. Thus, condition 3 in section 5 is not fulfilled. Yet there can still be some uncertainty in the applicability of TS theory when the reactants for Figure 16B,C are unsymmetrically substituted: Three possible transition states leading from V to B and  $B_1'$  in Figure 16B and to  $B_2$  in Figure 16C are the two dashed lines containing saddle points  $S_1$  and  $S_2$  and the dashed line joining  $R_1$  and  $R_2$ . We denote their free energies as  $G_{S1}$ ,  $G_{S2}$ , and  $G_{R1R2}$  and consider the case that

$$G_{S2} > G_{R1R2} > G_{S1} \tag{25}$$

In this instance, the transition state for the loss of V in a reaction originating from V in Figure 16B,C is principally the  $R_1R_2$  dashed line: The dashed line TS containing  $S_2$  has, we see from eq 25,





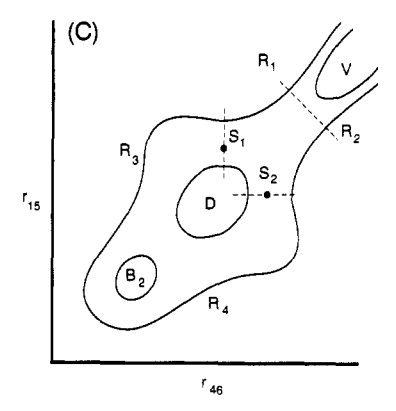


Figure 16. Contour plot for the Diels-Alder reaction (22)-(24), given by (A)-(C), respectively.

too high a free energy barrier to be the TS, and the TS containing  $S_1$  has too low a free energy to be a bottleneck. However, a fraction of the trajectories crossing the  $R_1R_2$  TS proceed along the  $S_2$  channel and are then reflected back to V. This fraction is not calculable from TS theory, and so the error in TS theory is small or large according as this fraction is small or large. Here, part of the TS  $R_1R_2$  is preempted by these largely unreactive trajectories which proceed into the  $S_2$  channel. In the case of reactions 8-10, instead, part of the TS for one reaction was preempted by another reaction. The error in each case, (22)-(24) or (8)-(10), depends on the amount of asymmetry of the flux at the bifurcation.

In summary, we have considered a situation where, at least as in Figures 8 and 9, the unusual event that the transition state of one reaction has been preempted by another has been explored, together with some possible topographical conditions for its occurrence and absence. We have also considered reactions, of which (22)-(24) are a prototype, where related problems can arise, depending on the detailed nature of the contour plot. A variety of examples are also given where the conditions in section 5 are not fulfilled, and so where TS theory is applicable.

Perhaps some of the potential complexities that may occur after obtaining detailed ab initio potential energy surfaces (pes) should be stressed. The presence of many coordinates not explicitly shown

<sup>(17)</sup> Borden, W. T.; Loncharich, R. J.; Houk, K. N. Annu. Rev. Phys. Chem. 1988, 39, 213.

<sup>(18)</sup> Houk, K. Private communication. I am indebted to Ken Houk for suggesting the coordinates in Figure 16.

might open up unsuspected pathways, pathways not easily seen perhaps in a pes projected onto a two-coordinate subspace. Again, alternative choices of coordinates for the describing a global picture in the two-coordinate subspace exist, and a choice among them needs to be made, initially on some intuitive basis perhaps. When a more complete pes is known, the choice can be made with the benefit of this added information. In addition to the topographical features considered explicitly in the present figures, there may be conical intersections, <sup>19</sup> and the sides of some hills may be shelves. <sup>20</sup> Some reactions may require three coordinates rather than two for a global picture, an example being the pseudorotation in an octahedral complex for which all exchanges of the ligands are possible. Such contours can perhaps be visualized on screens using three-coordinate plots.

The present article is intended to introduce the topic of global portrayals when alternative reactions and reaction paths exist. There remain various issues and perhaps some surprises which may emerge when the many-coordinate potential energy surfaces are calculated and the reaction paths and bifurcations obtained.

Acknowledgment. This research was supported by a grant from the National Science Foundation, and I am pleased to acknowledge its support. It is with a profound sadness that I dedicate this paper in this memorial issue to my colleague and friend for more than 30 years, Dick Bernstein. He stood and stands for all that is good in this scientific life—integrity, incisive thinking, vision, and a youthful joyousness in scientific inquiry. We all recognize that life has a natural limit, but it is when Nature takes a shortcut, as it did in Dick's case, that our sense of loss for all of us is the more acute.

## Appendix A. Behavior of Symmetric Stretching Coordinate in Figure 5 for the $X_3$ Reactions

We consider here the behavior of the symmetric stretching mode, so adjusted, along each of the three valleys in Figure 5, namely, along the negative  $S_{\rm Al}$  axis and along the radius obtained by rotating that semiaxis through an angle of 120° and then by rotating again through another 120°.

Along the negative  $S_{A1}$  axis,  $S_{A2}$  vanishes and so  $r_2$  and  $r_3$  are equal (eq 6). At  $S_{A1} = -\infty$ , it then follows from eq 6 that  $r_2 = r_3 = +\infty$ , and therefore, as seen from the definitions of the  $r_1$ 's in Figure 4a, this channel corresponds to the system being present as  $X^{(1)} + X^{(2)}X^{(3)}$ . Analogously, it is found that the channel in the upper left of Figure 3 corresponds to the system being in the form of the products of reaction 5a, while that in the upper right corresponds to the products of reaction 5b.

The variation in  $S_S$  with position in Figure 3 can now be immediately sketched along the above three directions (and calculated everywhere else numerically from a pointwise knowledge of  $r_1$ ,  $r_2$ , and  $r_3$  as functions of  $S_{A1}$  and  $S_{A2}$ .) The variation of  $S_S$  along this negative  $S_{A1}$  axis is obtained by expressing  $S_S$  in terms of  $S_{A1}$  along this path: Along the negative  $S_{A1}$  axis we have  $r_2 = r_3$ , and so eq 6 yields

$$S_{\rm S} + \sqrt{2}S_{\rm A1} = \sqrt{3}r_{\rm i}$$
  $S_{\rm A1} \le 0, S_{\rm A2} = 0$  (A1)

At the origin  $S_{A1}$  vanishes, while  $r_1$ , the bond length 1 in Figure 4a, changes relatively little from its equilibrium value in  $X_3$ . However, at  $S_{A1} = -\infty$ , the change in  $r_1$  is also small (the bond length of  $X^{(2)}X^{(3)}$  changes only slightly along this axis), and so eq A1 shows that  $S_S$  now equals  $+\infty$ . I.e.,  $S_S$  varies infinitely along this  $S_{A1}$  axis.

It is useful to rewrite eq A1 so that it is valid along the other two radial spokes obtained by rotating the  $S_{\rm A1}$  axis successively through 120° and 240°. Because of the  $C_3$  symmetry, we introduce for this purpose a radial coordinate  $S_{\rm R}$  defined by

$$S_{\rm R} = (S_{\rm A1} + S_{\rm A2})^{1/2} \tag{A2}$$

and rewrite eq A1 as

$$S_{\rm S} + \sqrt{2}S_{\rm R} = \sqrt{3}r(S_{\rm R}) \tag{A3}$$

where r is a function of  $S_R$  and equals  $r_1$  on the negative  $S_{A1}$  axis,  $r_2$  on the radial spoke obtained by rotating that axis clockwise through 120°, and  $r_3$  when the clockwise rotation is 240°. One can now see from eq 6 that since the lower bound to any  $r_i$  is only a relatively small negative value,  $S_S$  will always become infinite along those other two paths as the system separates into products.

### Appendix B. Behavior of Symmetric Stretching Coordinate for the X<sub>3</sub>Y Reactions along Particular Cylindrical Radii

We consider here the reaction 2, written now as

$$X_3Y \rightarrow X^{(i)} + X_2Y \quad (i = 1, 2, 3)$$
 (B1)

Along the  $S_{A2}$  axis, for the case of i=1 in reaction 8, we have  $r_2=r_3$ ,  $S_{A1}\geq 0$ ,  $r_1\rightarrow +\infty$ , and  $r_2$  remains small throughout (e.g., eq 6 and Figure 4b). It is then seen from eq 6 that both  $S_{A1}$  and  $S_S$  tend to  $+\infty$  as the reaction proceeds. There is, thereby, an infinite variation in the continuously adjusted  $S_S$  along this path. The relation between  $S_S$  and  $S_{A1}$ , obtainable from eq 6, expressed in terms of slightly varying  $r_2$  (= $r_3$ ), is given by

$$S_S - 1/\sqrt{2}S_{A1} = \sqrt{3}r_2$$
 (path for  $i = 1$ ) (B2)

At large  $X^{(1)}Y$  separation distances  $r_1$ ,  $r_2$  equals the equilibrium XY bond length in  $X_2Y$ ,  $r_{xy}(X_2Y)$ , the slope  $dS_S/dS_{A1}$  along the path is, asymptotically,  $1/\sqrt{2}$ , and the intercept  $S_S$  of this straight line at  $S_{A1} = 0$  is  $\sqrt{3}r_{xy}^e(X_2Y)$ .

The remaining two trigonally equivalent paths, in which i is 2 or 3, are obtained by rotating the path in eq B2 about the  $S_{\rm S}$  axis, perpendicular to the  $S_{\rm A1}$ ,  $S_{\rm A2}$  plane, clockwise through 120° for i=2 or 240° for i=3. An equation, obtained from eq B2, applicable to all three radial paths, and also useful in the immediate neighborhood of such radii, is

$$S_S = 1/\sqrt{2}S_R = \sqrt{3}r(S_R)$$
 (three paths) (B3)

where  $S_R$  is a cylindrical radius given by eq A3 and where

$$r(S_R) = r_i$$
 (i = 1, 2, 3 on the appropriate paths) (B4)

At large separations of  $X^{(1)}$  and  $X_2Y$  the slope  $dS_S/dS_R$  and the intercept  $S_S$  at  $S_{A1} = 0$  of the asymptotic straight line, seen from eq B3, has the values  $1/\sqrt{2}$  and  $r^e_{xy}(X_2Y)$  given earlier for the path for i = 1 in eq B2.

We consider next the reactions

$$X_3Y \rightarrow X_2 + X^{(i)}Y \quad (i = 1, 2, 3)$$
 (B5)

and first consider motion along the  $S_{A1}$  axis, but now for reaction B5 with i=1. During the course of this reaction,  $r_2$  becomes very large while  $r_1$  remains small and so now  $S_{A1}$  tends to  $-\infty$  (eq 6) instead of  $+\infty$ , while  $S_S$  still tends to  $+\infty$ . The relation between  $S_S$  and  $S_{A1}$  along the negative  $S_{A1}$  axis is best expressed, using eq 6, in terms of the now slightly varying  $r_1$ :

$$S_{\rm S} + \sqrt{2}S_{\rm A1} = \sqrt{3}r_{\rm I}$$
 (path for  $i = 1$ ) (B6)

The slope of this curve  $dS_S/d(-S_{A1})$  at large separation distances now equals  $\sqrt{2}$ , and the intercept of the latter line at  $S_{A1} = 0$  is  $\sqrt{3}r_1$ , i.e.,  $\sqrt{3}r_{xy}^e(XY)$ . Once again, for the other two paths related by a  $C_3$  symmetry about the  $S_S$  axis, the radius  $S_R$  given by eq A2 can be introduced. Instead of eq B6 we then have

$$S_S + \sqrt{2}S_R = \sqrt{3}\bar{r}(S_R)$$
 (all three paths) (B7)

where  $\bar{r}(S_R)$  denotes  $r_1$  on the first path,  $r_2$  on the path obtained by clockwise rotation through 120°, and  $r_3$  when the rotation is 240°. Equation B7 is again also useful in the neighborhood of these three radii.

<sup>(19)</sup> Xantheas, S.; Elbert, S. T.; Ruedenberg, K. Theor. Chim Acta 1991, 78, 365. Xantheas, S.; Atchity, G. J.; Elbert, S. T.; Ruedenberg, K. J. Chem. Phys., in press. Atchity, G. J.; Xantheas, S. S.; Ruedenberg, K. Ibid., in press. (20) Ruedenberg, K. Private communication.